


RESEARCH ARTICLE

Shared control methodology based on head positioning and vector fields for people with quadriplegia

Guilherme M. Maciel^{1*}, Milena F. Pinto² , Ivo C. da S. Júnior¹, Fabricio O. Coelho¹, Andre L. M. Marcato¹  and Marcelo M. Cruzeiro³

¹Department of Electrical Engineering, Federal University of Juiz de Fora (UFJF), Juiz de Fora, Brazil, ²Department of Electronics, Federal Center for Technological Education of Rio de Janeiro (CEFET-RJ), Rio de Janeiro, Brazil and ³Department of Clinical Medicine, Federal University of Juiz de Fora (UFJF), Juiz de Fora, Brazil

*Corresponding author. Email: guilherme.marins@engenharia.ufjf.br

Received: 25 March 2020; **Revised:** 24 April 2021; **Accepted:** 26 April 2021; **First published online:** 20 May 2021

Keywords: shared control, vector fields, mobile robots, head positioning, quadriplegia

Abstract

Mobile robotic systems are used in a wide range of applications. Especially in the assistive field, they can enhance the mobility of the elderly and disable people. Modern robotic technologies have been implemented in wheelchairs to give them intelligence. Thus, by equipping wheelchairs with intelligent algorithms, controllers, and sensors, it is possible to share the wheelchair control between the user and the autonomous system. The present research proposes a methodology for intelligent wheelchairs based on head movements and vector fields. In this work, the user indicates where to go, and the system performs obstacle avoidance and planning. The focus is developing an assistive technology for people with quadriplegia that presents partial movements, such as the shoulder and neck musculature. The developed system uses shared control of velocity. It employs a depth camera to recognize obstacles in the environment and an inertial measurement unit (IMU) sensor to recognize the desired movement pattern measuring the user's head inclination. The proposed methodology computes a repulsive vector field and works to increase maneuverability and safety. Thus, global localization and mapping are unnecessary. The results were evaluated by simulated models and practical tests using a Pioneer-3DX differential robot to show the system's applicability.

1. Introduction

Quadriplegia is a kind of paralysis caused by serious injury or illness. The quadriplegic patient has major sensory and motor deficits. The individual usually has visible contractions and regular movements of the shoulders and neck musculature [1, 2]. In this work, authors will focus on this type of individuals, that is, impaired individuals or paralysis of four main limbs [3], but capable of performing tilt movements with the head. Quadriplegia patients cannot use traditional motorized wheelchairs or wheelchairs that have joystick control. In this way, these patients require another kind of technology. Robotic systems are used in a wide range of applications, and such examples are in refs. [4, 5, 6]. For instance, they are also presented in independently daily activities [7]. Robotic devices are adopted in the assistive field and rehabilitation to enhance the quadriplegic people level of independence, social participation, and life quality [8, 9, 10, 11]. Physical assistance by using modern technology and robots is one of the most direct ways to help people with disabilities [2].

Unlike conventional motorized wheelchairs, Intelligent Wheelchair (IW) is a standard power wheelchair containing a sensor or a mobile robot base to which a seat has been attached. This kind of system provides navigation assistance to the user in different levels of applications [12]. Hence, IW arises as a kind of robotic rehabilitation system by equipping a wheelchair with original mobile robotic technologies [13]. A smart wheelchair is an active topic, as shown in the review presented by ref. [14].

There are several types of IW controllers for quadriplegic people. These controllers are called hands-free, and they can be used in different ways, such as tongue movements, eye tracking, voice commands, electrograms, facial recognition, and head inclination [15]. Note that the choice of human interface machine (HMI) should consider the level of disability to give autonomy to the user.

An important subject related to IW is the control strategy. The shared control is a necessity to increase process reliability while avoiding obstacle hitting. The wheelchair control is shared by the user and the embedded intelligent system. The user indicates where to go, and the system performs obstacle avoidance and planning. However, due to the physical limitation of quadriplegic users, wheelchair control turns to a complex task, where a simple displacement among places becomes a difficult task. The assistive robotics (AR) have developed interfaces, electronics devices, and shared control strategies to overcome a few of these issues, such as in refs. [16, 17] and [13]. Some research works with shared wheelchair control tried to infer the driver's intention for decision-making [18]. This work utilizes shared control through a vector obstacle avoidance field, where the driver has its autonomy of choice, but the wheelchair creates a safe environment for locomotion. The most common task of a shared control system is obstacle avoidance. A technique widely used for avoiding collisions is the artificial potential fields (APF), which uses virtual repulsive forces between the obstacles and the robot based on distance.

1.1. Main contributions

This research proposes a low-cost system with an easy, confident, and comfortable interface for people with quadriplegia, where mapping and localization are unnecessary. The focus is on avoiding nonintentional collisions, which may increase maneuverability and accurate pattern recognition of each user. As the shared control system routes are defined according to the user's desire, the results were based on the routes' qualitative analysis. From the results, it was possible to see the ease of control in deviations from obstacles and narrow passages. Besides, the experiment was counted on volunteers' participation in a simulator test, evaluating their perception and degree of difficulty. Such tests also provided quantitative data on manipulating the control system in the performed route. The main contributions can be summarized as follows:

- An interface based on head movements that use seven discrete commands to simplify the navigation. These commands are the classification results of the smooth head movements.
- A supervisory system that computes vector fields from a depth camera data to ease the navigation. The methodology compensates for the obstacle width and IW dimensions. Note that this system does not prevent collisions. Thus, the user's displacement intentions are sovereign throughout the process.

1.2. Organization

The remainder of this research is organized as follows. Section 2 discusses the technologies and the main techniques used in AR. Section 3 details the project development emphasizing the main algorithms presented in the proposed methodology. Section 4 presents the results in both simulated and real environments to show the system's performance. Finally, Section 5 presents conclusions remarks, and future works.

2. Background and related works

2.1. Hands-free controllers

In several works, the desired motion intention is estimated from the orientation of the user's face. Such as in ref. [19], the semi-autonomous navigation is performed using localization based on 3D-Scanner and RGB camera. In Pereira et al. [15], two types of wheelchair controls are compared using facial recognition: (i) the Joyface emulate an analog joystick based on the head tilt and (ii) the Intel RealSense SDK

that controls the IW using facial expressions. Even with higher demands for physical effort, volunteers considered performing head movements more comfortable and safer than facial expressions. However, the authors applied both types of controllers to individuals capable of using them efficiently.

As mentioned before, tongue movements utilization is another option. The authors of ref. [20] developed the Tongue Drive System, where the participant uses a metallic piercing in the tongue. Magnetic sensors, which are closer to the cheek, recognize the position of the piercing to classify the control action. In this context, advances in the area of speech recognition have been increasing the accuracy of IWs controlled by voice. In this interface, the user pronounces phrases to configure and operate the system. The most widely used recognition algorithms are the Hidden Markov Model and Artificial Neural Networks. Voice recognition can be performed by specialized hardware or by software [21].

A system often used in smart wheelchair interfaces is electrography. This interface uses muscle contractions (EMG) or electrical signals from the brain (EEG) when the movements present extreme limitations. For instance, in the work of Liu et al. [22], the authors proposed a combination of APF and EEG signals to perform motion commands in unstructured environments. Different strategies also allow the measurement of spontaneous EEG signals in more adverse conditions [23]. The neck movement may be used depending on the quadriplegic disability degree. For instance, some works used inertial measurement unit (IMU) to measure the inclination and angular changes of the head. In Rohmer et al. [24], the user moves the head to control the pointing of a laser on the ground. A camera captures this position, and the system navigates autonomously to this point. The IMU can also act directly at the IW speed, using proportional pitch movement to move forward/backward and roll right/left [25]. This kind of interface is called Head-joystick. Another possibility to control the wheelchair by using head movements is to use discrete commands. The authors in ref. [26] studied pattern recognition techniques to classify the actual head inclination. Their focus was on classification, and they used only five classes.

According to Torkia et al. [27], motorized wheelchair users typically complain about the difficulty in climbing ramps, moving in small spaces, crossing doors, and avoiding obstacles. Due to the limitations involved in hand-free interfaces, it is strictly necessary to use shared control to ensure safe navigation. The user makes the decisions, and a supervisor system assists in the tasks.

2.2. *Intelligent wheelchairs*

Different solutions for wheelchair alternative controls have been proposed in the literature. For instance, Chauhanet et al. [28, 29] proposed a new model using voice commands for controlling the wheelchair. As a drawback, this kind of interface is subject to environmental noises. The works of Huo and Ghovanloo [30] and Kim et al. [20] implemented a tongue drive system to control a motorized wheelchair, and they tested only in volunteers with spinal cord injury (SCI). A controller for assistive robots through small face's movements or limbs was proposed by Rohmer et al. [24]. The authors used electromyograph (EMG) and signals generated by brain activities through electroencephalograph (EEG). The navigation strategy is presented by an IMU that tracks the user's head posture. This system is not comfortable for the user. Gajwani and Chhabria [31] controlled a wheelchair by eye-tracking and eye-blinking obtained by a camera. The performance of this system is hugely affected by illumination, brightness, and camera position.

An interesting technique for controlling the wheelchair is learning by demonstration (LbD). In the work of ref. [32], the authors adopted the user modeling approach to model the assistant's behavior. In this way, the IW learns the assistive policy through dynamically coupled demonstrations given by a remote human assistant. A similar idea is given by Kucukyilmaz et al. [33]. As a drawback of the LdD methodology, the user should use the hands to move a joystick, demonstrating to be an unfeasible solution to quadriplegia users. Head gesture-based interaction interface has been used in some IW systems [34, 35]. Most of the researches discuss how to construct and receive environmental information, such as in Ruzaij et al. [34]. A few types of research explored face detection and direction recognition [35, 36], but the movement of the user's head is not considered, usually being extensive movements.

Therefore, this work is concerned with the movement of the operator's head, generating shorter and more comfortable movements. The work of Teodorescu et al. [37] proposed here a stochastic dynamic programming approach where the user's intention is estimated using Markov chain modeling. However, the results were only formulated and validated in simulation.

In relation to the control methodology, the shared control wheelchair provides personalized assistance to its user. Besides, it provides safety due to its obstacle avoidance strategy. The research of Triharminto et al. [38] proposed an approach to integrating the APF and control systems under nonholonomic constraints. In Seki et al. [39], the body is modeled as a rectangular format, and the repulsive field was calculated considering the front and back. This turned the method more effective. Another solution to improve the obstacle avoidance considering the geometry was presented in ref. [40]. It was proposed an adaptation of the APF where several range finder sensors were spread over all of the wheelchair sides.

In the context of semi-autonomous navigation, the work of Olivi et al. [41] proposed a new technique to avoid obstacles based on vector fields. The method uses a discrete control system with an EEG interface where the user chooses the direction of the movements. In parallel, the intelligence uses a laser scan to compute vector fields from obstacles ahead and contribute to a safe path. The proposed research work modifies this methodology to apply it in the developed interface. Similarly, the work of Wang et al. [42] had a semi-autonomous routine called smart motion controller (SMC). The user was responsible for choosing all the movements. But, if a collision is imminent, the commands block the movement. Due to the price of scanning lasers, several works have been choosing the utilization of cameras. Besides, these sensors can obtain distance from obstacles and recognize environmental standards. For example, the shared control systems in refs. [43] and [44] used cameras RGB-D for obstacle avoidance, mapping, and localization.

Differently from the proposition of this research, the authors of ref. [45] presented a solution that helps patients with spinal cord injuries using a wheelchair with a robotic arm. From HMI, the subjects selected eight movements that the wheelchair can execute. Signals EOG (i.e., electrooculogram) are detected by electrodes attached to the surface skin. The eye blinking selects a move and other functions given by HMI. The authors analyzed the amplitude of the EOG signal to identify the correct correspondence of eye blinking. The absence of a shared control added to the difficulty of quick selections by the user can cause problems during the movement of the wheelchair. The work of Qassim et al. [46] proposed a practical wheelchair control using face tilting (i.e., neck movement). The face tilt is detected by a camera connected to a computer for image processing. This approach requires a satisfactory ambient lighting condition to be efficient. The method does not identify the subject, only the face that appears closest to the image. Thus, this characteristic can cause problems during the operation.

As can be seen, most of the works do not present all the pertinent steps in the control of the smart wheelchair. Some of them focus on the control strategy, while others focus on the device to control the wheelchair or in the head movements classification. This research shows the head-gesture sensor, the head movements' classification, the shared control strategy, as well as results with different users to evaluate the proposed approach. For instance, Table I shows the differences among the similar mentioned works and the methodology proposed by this research. Note that the symbol "-" is used when the work does not apply or does not mention this step. Note in this table that the Joysticks are the most common method. However, they are somehow limited. Also, notice that not all methods have shared control strategies and that the proposed method supports a larger number of commands.

3. Project development

3.1. Head-keypad interface

In literature, many projects use a head movement interface that operates simulating an Analog Joystick (i.e., Head-Joystick). The velocity values are directly connected to the magnitudes of the inclination angles of the head. The user must continuously adjust the positioning of the head during navigation

Table I. Comparison with similar works.

| Works from literature | IW controllers | Shared control | Head Mov. | Movement classification | Designed for quadriplegia? |
|------------------------|------------------|--------------------------------|-----------|-------------------------|----------------------------|
| Ruzajic et al. [34] | IMU+Voice | – | 4 | HMM + DTW ¹ | Yes |
| Dey et al. [35] | Accelerometer | – | 5 | – | Yes |
| Jia et al. [36] | Camera | – | 5 | Adaboost + Camshift | Yes |
| Teodorescu et al. [37] | Joystick | Stochastic Dynamic Programming | – | – | No |
| Wang et al. [42] | Joystick | SMC | – | – | No |
| Tomari et al. [43] | Camera, Joystick | Vector Fields | 3 | Face API | No |
| Huang et al. [45] | Electrooculogram | Stochastic | – | – | Yes |
| Qassim et al. [46] | Camera | – | 3 | Not Specified | Yes |
| Proposed Metodology | IMU | Vector Fields | 7 | Mahalanobis | Yes |

¹Dynamic Time Warping.**Table II.** Acting classes.

| Class | Action |
|-------|------------------------|
| ↑ (1) | Linear forward motion |
| ↓ (2) | Linear backward motion |
| ↷ (3) | Right rotation |
| ↶ (4) | Left rotation |
| ↗ (5) | Right curved movement |
| ↖ (6) | Left curved movement |
| ◇ (7) | Stopped |

according to the desired velocities. The Head-Keypad interface proposed in this research is based on previous studies performed by the authors in ref. [26]. However, differently from this previous work, this research presents an interface for seven discrete movements as well as a shared control strategy. This HMI aims at classifying the current positions of the user's head to perform movements in the IW. This framework works discretely as a person pressing the buttons of a keyboard. The justification is related to comfort and ease. The user should only tilt the head slightly in the desired direction. Then, the classifier recognizes the movement's intention. As long as the head positioning is in the desired command class, the intelligence involved decides the speed values to respect the movement decision, and at the same time, to facilitate the obstacle avoidance.

This HMI significantly reduces the physical effort made by the user. The seven possible user's actions are presented in Table II and Fig. 1. Note that the class 7 is the natural positioning of the head when the chair is in a stationary position.

3.1.1. Head tilt sensing

The IMU on the top of the user's head classifies the movements based on the measured angles. The sampled data refer to the angles roll and pitch of the user's head frame, as shown in Fig. 2. The prototype consists of IMU model GY-521 and a microcontroller ATmega. The equipment is inserted on top of the headset, as illustrated in Fig. 2.

The microcontroller reads the Euler Angles and applies a Kalman filter [47] to provide the roll and pitch angles (i.e., ϕ representing roll and θ representing pitch) concerning the global frame (ϕ_f , θ_f).

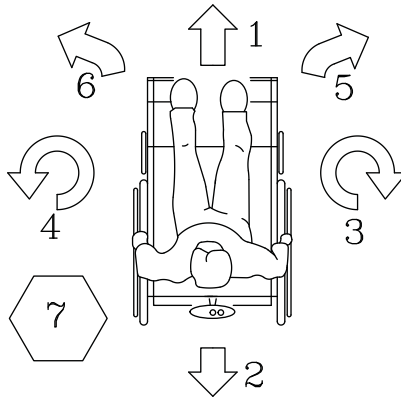


Figure 1. Acting classes.

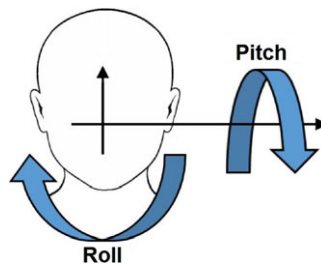


Figure 2. Head frame and angles.

The user must start the system in a neutral position. At this moment, the inertial frame is computed (ϕ_N, θ_N) . This process will make the neutral position of the user as the origin of the new system. The head inclination is computed in this reference. Each user has a natural tilt of the head, and the IMU can be positioned in different ways. This procedure is used in both training and operation. Finally, the current user angles are computed, Eq. (1). These angles are used for data training and classification.

$$\begin{bmatrix} \phi_U \\ \theta_U \end{bmatrix} = \begin{bmatrix} \phi_f - \phi_N \\ \theta_f - \theta_N \end{bmatrix} \tag{1}$$

3.1.2. Pattern recognition

The user has a unique physical condition. Thus, a training phase is required for each individual. For each class, the user should lightly place the head in a certain way, as shown in Fig. 3. During the training, the user is asked to perform several random transitions, that is, five times for each class, which is required once the angles can suffer variations for the same category at different times. It is desired to obtain the probabilistic dispersion of the data in the *roll – pitch* plane.

The gyroscope presented in the IMU recognizes the transients to collect data only with the head in the position stop. After each movement, the system receives new 100 points to the training set (i.e., 3500 data samples in total). The Mahalanobis Distance method was chosen for the classifier because of the good cost–benefit about accuracy and complexity for this kind of application [26]. When a new input consisting of $\mathbf{x} = [\phi_U, \theta_U]^T$ in radians, the seven distances of Mahalanobis are calculated, according to Eq. (2), using the mean vector $\boldsymbol{\mu}$ and covariance matrix \mathbf{S} of each n class. The data will belong to the shortest distance class.

$$D_{M[n]}(\mathbf{x}) = \sqrt{(\mathbf{x} - \boldsymbol{\mu}_n)^T \mathbf{S}_n^{-1} (\mathbf{x} - \boldsymbol{\mu}_n)} \tag{2}$$

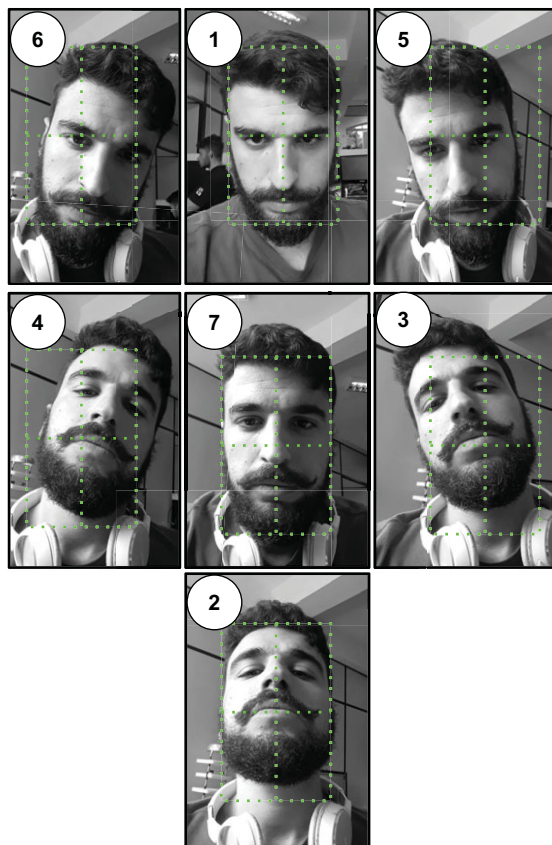


Figure 3. Head tilt pattern for each class.

3.2. Vector fields

According to ref. [48], many collision avoidance algorithms have been proposed in the literature. For instance, the Artificial Potential Field (APF) algorithm [49] is used to find the shortest path between two points. However, this approach is very sensitive to a local minimum in the case of an asymmetric environment. Regarding the Bug algorithm, the robot follows the boundary of each obstacle in its way until the path is free. However, it does not consider any other obstacles during the edge detection process, which reduces crash reliability. The vector field is a real-time obstacle avoidance method that uses the two-dimensional Cartesian. Note that a great advantage is a possibility of turning the APF to the robot's controller. Besides, APF is fast enough to be applied onboard of mobile robots in real-time, and it is well applied in the robotics field, as shown in refs. [50, 51] and [52]. In order to overcome many of these issues, a shared control strategy is proposed. In this shared strategy, the speed of the chair is controlled when approaching objects. This will not entirely avoid incoming obstacles. However, it will help the user prevent them by taking some of the control burdens, which is similar to a change in the keypad sensitivity when approaching objects to allow more accurate maneuvers.

The shared control is based on vector fields, carrying information about the obstacles detected near the robot. Moreover, the vector fields work together with the Head-Keypad in the decision-making of the angular and linear speeds. The exteroceptive sensor identifies obstacles using an RGB-D Camera above the user's head. The image is transformed into a 2D rangefinder to provide the planar location of the points concerning the camera frame. Every detected obstacle contributes to a repulsive vector. To better perform the field, the robot is not considered as a dimensionless point. The wheelchair dimensions are

Table III. Distance and angulation computing.

| Region | Limits | d_i | λ_i |
|--------|---|--|--------------------------------------|
| 1 | $x_i \leq x_w$ $y_i < -y_w$ | $-y_i - y_w$ | $-\pi/2$ |
| 2 | $x_i > x_w$ $y_i < -y_w$ | $\sqrt{(x_i - x_w)^2 + (y_i + y_w)^2}$ | $\text{atan2}(y_i + y_w, x_i - x_w)$ |
| 3 | $x_i > x_w$ $-y_w \leq y_i \leq y_w$ | $x_i - x_w$ | 0 |
| 4 | $x_i > x_w$ $x_i > x_w$ | $\sqrt{(x_i - x_w)^2 + (y_i - y_w)^2}$ | $\text{atan2}(y_i - y_w, x_i - x_w)$ |
| 5 | $x_i \leq x_w$ $y_i > y_w$ | $y_i - y_w$ | $\pi/2$ |

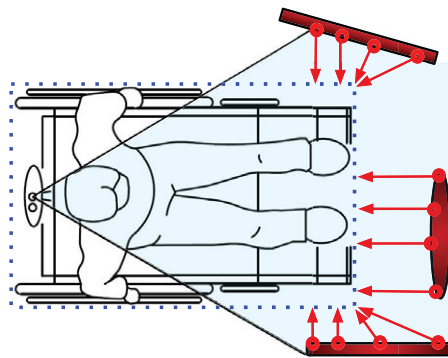


Figure 4. Individual repulsive fields per obstacle.

modeled as a rectangular body, and any structure must be contained in this rectangle. The action points of the repulsive forces coming from the obstacles are computed on the edges of the rectangle. The distance and direction for the field calculation consider the point closest to the obstruction. This point belongs to any of the edges, as shown in Fig. 4.

3.2.1. Field calculation

The Cartesian coordinates $[x_i, y_i]$ of the observed obstacles in respect to the robot frame are necessary for this calculation. The more distant coordinates from the surface of the rectangle (i.e., more distant than maximum distance R) are discarded. The fields are calculated based on the distances from the obstacle to the edge d . They also consider the incidence angle of λ_i . The distance y_w is half the width of the IW. The parameter x_w is the distance from the origin of the frame to the front. Table III exhibits the distances and orientation calculation for different regions of obstacles. Figure 5 presents an example.

The repulsive field \vec{C} is calculated by Eq. (3), through the contribution of the five obstacle regions. The variable β_j is the gain of the respective region. The variables n_j are the total of obstacles within the limit, that is, $d_i < R$. Thus, it is possible to customize the risk of each region and compensate for different obstacle widths.

$$\vec{C} = \sum_{j=1}^5 \sum_{i=1}^{n_j} \frac{-\beta_j}{(n_j + 1)d_{j,i}} \begin{bmatrix} \cos(\lambda_{j,i}) \\ \sin(\lambda_{j,i}) \end{bmatrix} \tag{3}$$

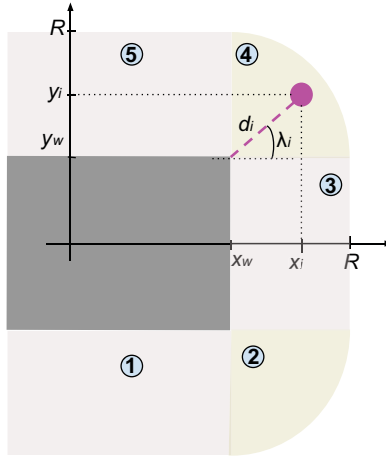


Figure 5. Obstacle modeling.

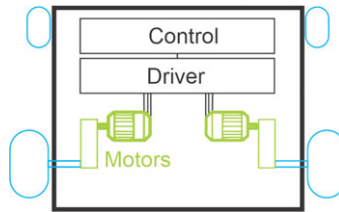


Figure 6. Wheelchair motor arrangement.

3.3. Wheelchair model

The wheelchair model used in the simulations consists of a dual actuated system. This chair has the same kinematic model developed by ref. [37]. Such a chair’s behavior is very similar to manual ones and should feel natural to the individual. Figure 6 shows a representation of the wheelchair model. Note that commands can be easily translated in this type of system to control wheelchair angle and linear speed. For example, pure rotation in the central chair axis can be obtained by turning motors in opposite directions with the same speed. In the same sense, pure linear movement by rotating the engines in the same direction and speed.

As previously described, pure rotation and linear motion are simply obtained. However, the curve around a given point has to be modeled in more detail. This motion model can be described as in Fig. 7. In this, the chair turning angle c_{ang} can be calculated as a difference between the arc radius formed by the right tire R and the left tire L divided by the chair length CL , that is, $c_{ang} = \frac{R-L}{CL}$.

3.4. Shared speed control

Three control vectors with origin in the robot’s center govern the velocities: the linear velocity vector \vec{v} , the right turn vector \vec{s}_r , and left turn vector \vec{s}_l . According to the user’s move decision, the wheelchair will assume linear velocity proportional to \vec{v} and angular velocity according to the right and left turn vectors (i.e., angles θ_r and θ_l). These angular velocities form \vec{s}_r and \vec{s}_l , respectively.

Before the navigation, the default vectors ($\vec{v}^{(d)}$, $\vec{s}_r^{(d)}$, and $\vec{s}_l^{(d)}$) need to be defined. When there is no repulsive field, they command the velocities. The field \vec{C} interacts with the default vectors. Besides, it changes velocities to perform the obstacle avoidance safely. This process produces vectors \vec{v} , \vec{s}_r , and \vec{s}_l . Figure 8 illustrates this operation and shows all involved variables.

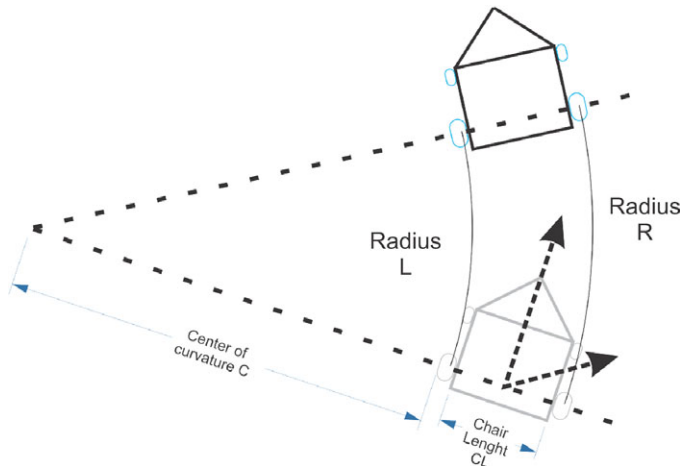


Figure 7. Movement model.

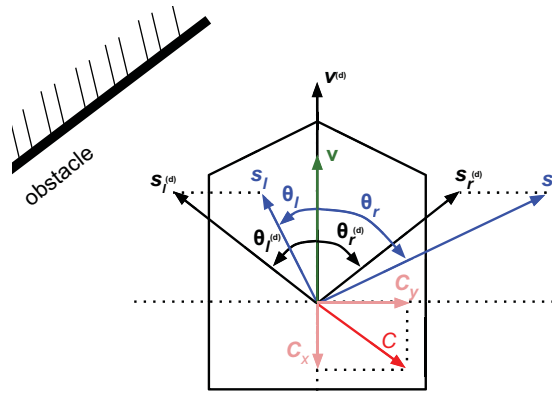


Figure 8. Vector field actuation.

The repulsive field is composed of the robot frame’s orthogonal components, where \vec{C}_x acts on the linear velocity and \vec{C}_y on the angular vectors. \vec{C}_x is added to $\vec{v}^{(d)}$ to decrease the linear velocity proportionally to front obstacles distribution.

$$\vec{C} = [C_x, C_y]^T = \vec{C}_x + \vec{C}_y \tag{4}$$

$$\vec{v} = [v_x, 0]^T = \vec{v}^{(d)} + \vec{C}_x \tag{5}$$

The vector \vec{C}_y will be added to the default angle vectors. Equation (7) calculates the angles with the new \vec{s}_r and \vec{s}_l . These angles will increase or decrease according to the lateral distribution of the obstacles.

$$\vec{s}_{r,l} = \vec{s}_{r,l}^{(d)} + \vec{C}_y \tag{6}$$

$$\theta_{r,l} = \text{acos} \left(\frac{\vec{s}_{r,l} \vec{v}}{\|\vec{s}_{r,l}\| \|\vec{v}\|} \right) \tag{7}$$

The user’s motion intention is sovereign to the repulsive field. Even close to the obstacle, the IW will not go against the user’s decision. Thus, this work does not completely prevent collisions. The system only saturates the velocities with minimum values to ease the navigation and to avoid nonintentional collisions. Table IV shows the velocity classes.

Table IV. Final velocities.

| Class | Linear velocity (v) | Angular velocity (ω) |
|-------|--------------------------------|---|
| ↑ (1) | $\max(v_{\min}, \alpha_1 v_x)$ | 0 |
| ↓ (2) | $-v_{\min}$ | 0 |
| ↷ (3) | 0 | $\min(-\omega_{\min}, \alpha_2 \theta_r)$ |
| ↶ (4) | 0 | $\max(\omega_{\min}, \alpha_2 \theta_l)$ |
| ↗ (5) | $\max(v_{\min}, \alpha_3 v_x)$ | $\min(-\omega_{\min}, \alpha_4 \theta_r)$ |
| ↖ (6) | $\max(v_{\min}, \alpha_3 v_x)$ | $\max(\omega_{\min}, \alpha_4 \theta_l)$ |
| □ (7) | 0 | 0 |

The maximum and minimum functions guarantee the sovereignty of the user's decisions. The four ($\alpha_1, \alpha_2, \alpha_3$, and α_4) constants must be set according to the performance and mission security. For linear backward motion, the IW assumes a minimum value due to the visibility and sense of the task. It only should be used in deadlock situations. It is worth emphasizing that curved movements are not considered when the wheelchair is moving backward. The reason relies on the lack of the user's field of view, which can interfere with its safety.

4. Results and discussion

The first part of the results is dedicated to evaluate the quality of command pattern recognition and to study all the gains involved in the shared control. Besides, the experimental tests will prove the effectiveness of the proposed interface. All results use the real prototype, a microcontroller, an IMU, and a Bluetooth module.

4.1. Preliminary study

The user's Head-Keypad interface should be calibrated. This process results in the scenario like that shown in Fig. 9. The scenario contains the training data and the discriminated region of the Mahalanobis Classifier. The colors are the actual class of the user's head. It is important to note that smooth movements were performed with little amplitude once the user's comfort is one of the focuses of this work.

The preliminary tests and the tuning of all the parameters were performed using a simulated IW model in MATLAB[®]. After several trials involving many possibilities of obstacles, the gains of the repulsive field β , the velocity gains α , and the default vectors were chosen empirically. The test of the pathways was carried out to evaluate the pattern recognition and the shared control of velocities jointly. This research work has developed a real HMI to control the simulated robot. The interface receives information ϕ_U and θ_U of the prototype. Figure 10 shows two of the tests.

4.2. Experimental evaluation

4.2.1. Gazebo platform

A virtual environment was created in Gazebo software containing several obstacles, narrow spaces, and a realistic IW. This wheelchair model, developed by ref. [53], features a front-wheel-drive and an RGB-D camera above the back. The Robotic Operating System (ROS) was chosen as a meta-operating system since it is an open-source platform. This operating system assists in robot application development and promotes code reuse. Figure 11(a) illustrates the environment. Figure 11(b) presents the registered behavior of the variables. During the path, the user deviates from objects at the beginning and navigates throughout the room to show the system's operations. Note that the elements in the room are not visible in this figure. The details can be analyzed by the video: <https://youtu.be/hwD4wD8oJro>.

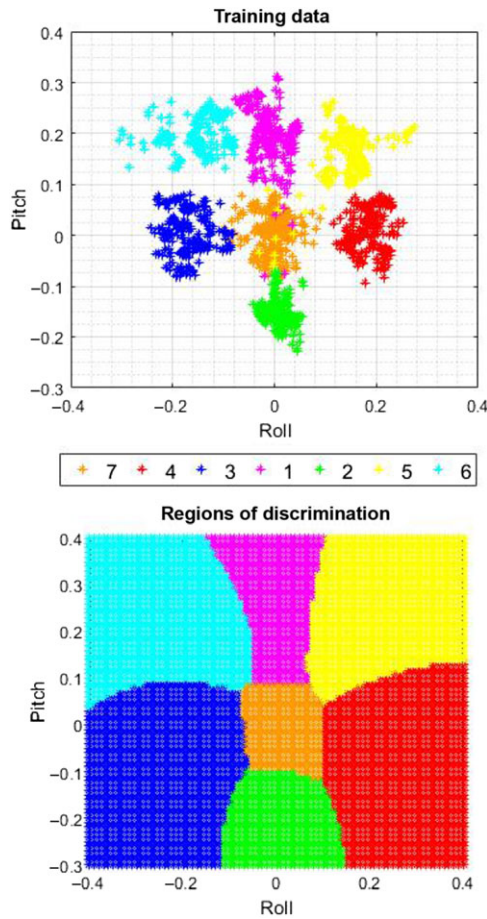


Figure 9. Mahalanobis classification.

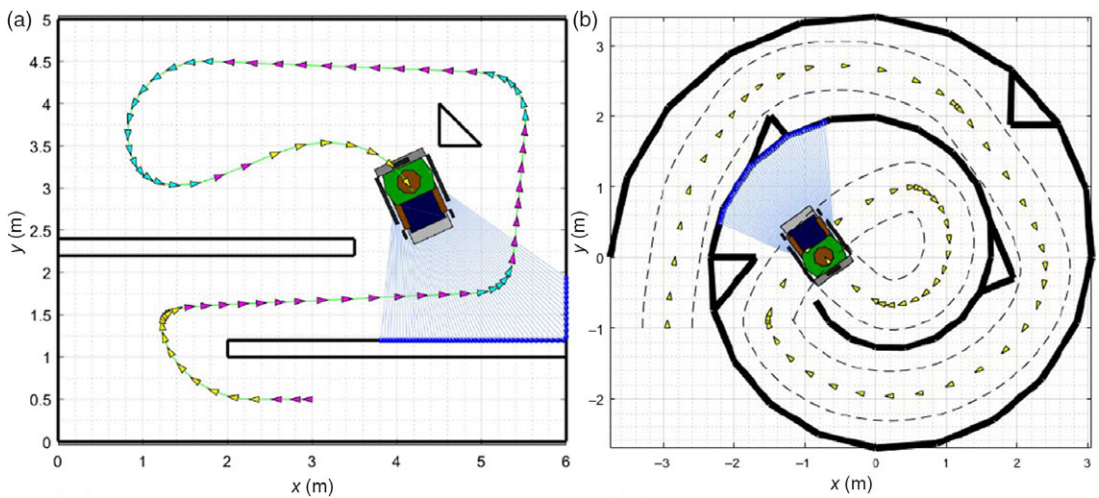


Figure 10. Simulation 1. (a) A journey through narrow aisles and obstacle diversion. It took only nine head movements, and it was necessary to use only classes 1, 5, and 6. (b) Spiral journey without commands changes.

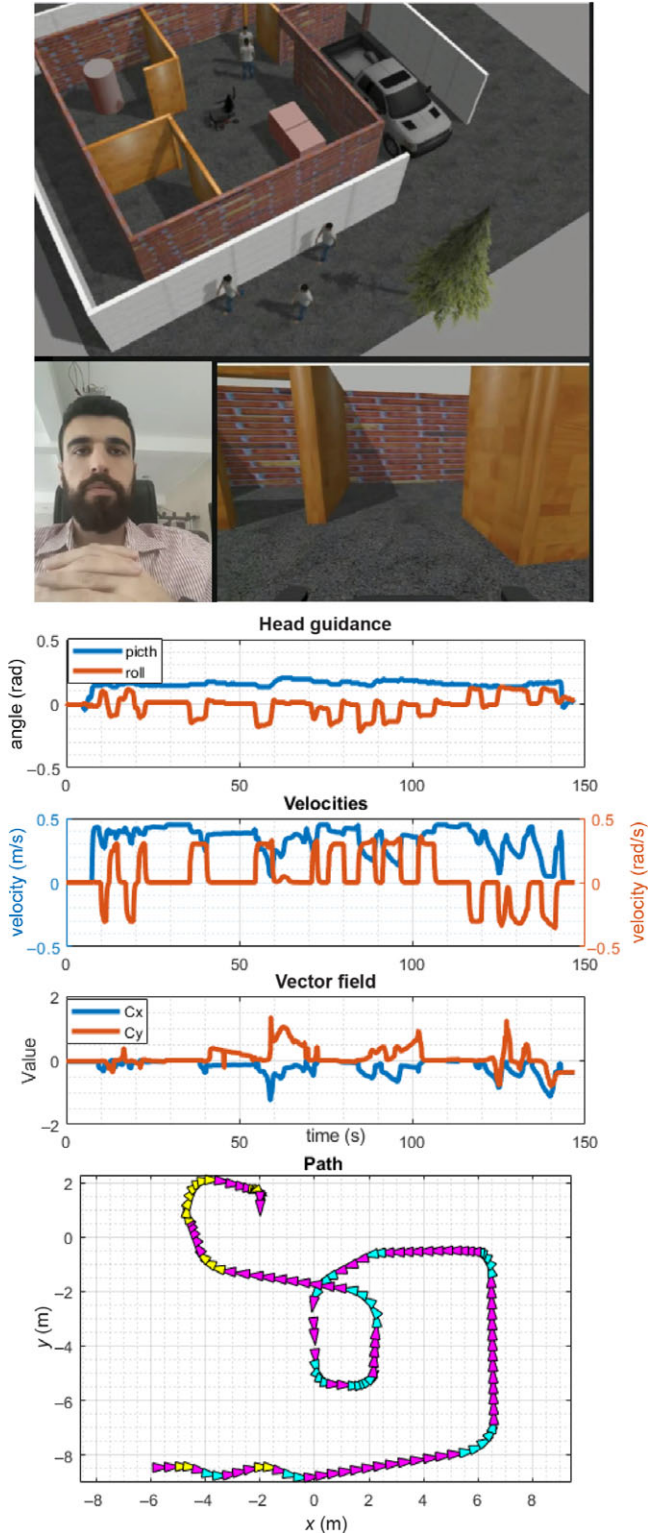


Figure 11. Experimental evaluation. (a) Virtual environment. (b) Registered results.

Table V. Volunteers statistics (for circuit).

| | Mean | Best | Worse | σ |
|----------------------------------|-------|------|-------|----------|
| Head command changes | 44.86 | 27 | 61 | 10.45 |
| Angular direction changes | 8.67 | 5 | 19 | 4.12 |
| Absolute head displacement (rad) | 9.29 | 3.66 | 15.6 | 4.04 |
| Deadlocks | 0.15 | 0 | 2 | 0.47 |
| Time (s) | 110 | 98 | 140 | 10.68 |

Table VI. Volunteers opinion.

| Item | Endpoints | Mean | Best | Worse | σ |
|-----------------|---------------|------|------|-------|----------|
| Mental Demand | 1–10 low-high | 1.84 | 1 | 4 | 0.89 |
| Physical Demand | 1–10 low-high | 2.15 | 1 | 4 | 0.98 |
| Temporal Demand | 1–10 low-high | 2.61 | 1 | 5 | 1.19 |

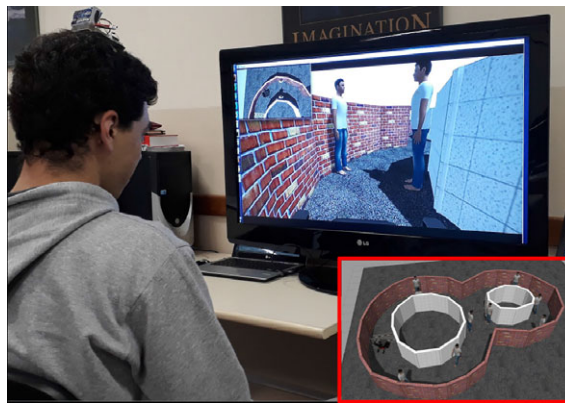


Figure 12. Setup for the volunteers test.

Another experimental evaluation was performed to assess the proposed interface. In this test, 20 volunteers used the Head-Keypad to guide the simulator in an eight shape circuit with obstacles. Figure 12 presents the setup for the volunteers. The procedure consisted of (i) assembling the Mahalanobis classifier, (ii) a practice round, and (iii) three rounds of analysis. The obtained results were divided into two main aspects. The first one regards the effectiveness of the methodology: (i) total command changes, (ii) curve direction changes, (iii) the absolute angular displacement traveled by the head, (iv) deadlocks that resulted in stopping the IW and performing unexpected maneuvers, and (v) round times. (i.e., Table V. The second result (i.e., Table VI is about subjective parameters from the user (e.g., mental demand). For this task, the questionnaire NASA Task Load Index (NASA-TLX) [54] was partially applied for each of the volunteers.

Table V suggests that some of the required commands change significantly from one user to another, given the significant value of variance about the mean value, which is an indication that some users may adapt to the system faster while others may require more time. Although some users have a higher number of maneuvers, the absolute displacement has a low value even when considering the worse case. Note that the volunteers did not have previous training. The mental demand in Table VI is more

correlated to the number of commands and directions changes once the volunteer makes decisions. Note that the low number of deadlocks also indicate that the system is easy to use, but still require some adaptation. The low mean value and σ also means that the system has low demand requirements. The authors also calculated that the significance of obtaining a value three or better is 96%, meaning that the test is significant in its context. Despite the results, the authors understand that randomized tests would be better to evaluate this type of situation.

4.2.2. *Real test environment*

It is common to test methodologies for intelligent wheelchairs in commercially differential robots in order to analyze the behavior in real physical systems [41, 55]. A small environment was set up to carry out the test using the Pioneer-P3DX robot. The robot was controlled from outside the environment. This robot is controlled by a Raspberry Pi 3 and sensed by a depth camera Asus XtionPRO. The mission was recorded in the first and third person and is available in <https://youtu.be/fydTb9-qug8>.

It is essential to mention that the depth camera cannot identify measurements below 40 cm, making the application in the P3DX less efficient compared to an IW. Smaller robots will reduce the influence of lateral vector fields. Even so, the methodology can be successfully proven in this scenario.

5. Conclusions and future work

This research presented a low-cost solution for IW applications. An interface for people with tetraplegia called Head-Keypad was developed based on slight neck movements. The IMU classifies the current inclination of the head in seven different performance classes. The Mahalanobis distance classifier indicated good accuracy for the context.

Due to cost–benefit reasons, this work uses a depth camera instead of a laser scan. Even with a reduced field of vision, the proposed methodology was proved. In the developed shared control system, the user determines the movement direction. The proposed intelligent system decides the magnitude of IW velocities based on repulsive vector fields. A few extensions are foreseen in this research work. First, the system will be implemented in a real IW. Therefore, it is also intended for a further study with tetraplegic users. The degree of mobility and the performance of these patients can be analyzed in the experiments proposed in these tests.

Acknowledgments. The authors would like to thank CNPq, CAPES, Fapemig, UFJF, CEFET-RJ, and INESC Brazil for supporting this research work.

Conflicts of Interest. Conceptualization, methodology, and writing Guilherme M. Maciel, Milena F. Pinto, and André L. M. Marcato; review and editing Fabrício O. Coelho and Marcelo M. Cruzeiro.

References

- [1] C. Fattal, V. Leynaert, I. Laffont, A. Baillet, M. Enjalbert and C. Leroux, “Sam, an assistive robotic device dedicated to helping persons with quadriplegia: Usability study,” *Int. J. Soc. Rob.* **11**, 1–15 (2018).
- [2] H. Jiang, B. S. Duerstock and J. P. Wachs, “Variability analysis on gestures for people with quadriplegia,” *IEEE Trans. Cybern.* **48**(1), 346–356 (2016).
- [3] M. A. Kader, M. E. Alam, N. Jahan, M. A. B. Bhuiyan, M. S. Alam and Z. Sultana, “Design and Implementation of a Head Motion-Controlled Semi-Autonomous Wheelchair for Quadriplegic Patients Based on 3-Axis Accelerometer,” *2019 22nd International Conference on Computer and Information Technology (ICCIIT)* (2019) pp. 1–6.
- [4] D. M. Wolpert, K. Doya and M. Kawato, “A unifying computational framework for motor control and social interaction,” *Philos. Trans. R. Soc. London Ser. B Biol. Sci.* **358**(1431), 593–602 (2003).
- [5] Y. Hirata and K. Kosuge, “Distributed Robot Helpers Handling a Single Object in Cooperation with a Human,” *Proceedings 2000 ICRA. Millennium Conference. IEEE International Conference on Robotics and Automation. Symposia Proceedings (Cat. No. 00CH37065)*, vol. 1 (2000) pp. 458–463.
- [6] W. A. Neto, M. F. Pinto, A. L. Marcato, I. C. da Silva and D. d. A. Fernandes, “Mobile robot localization based on the novel leader-based bat algorithm,” *J. Control Autom. Electr. Syst.* **30**(3), 1–10 (2019).

- [7] A. Saxena, J. Driemeyer and A. Y. Ng, "Robotic grasping of novel objects using vision," *Int. J. Rob. Res.* **27**(2), 157–173 (2008).
- [8] R. Gelin, J. Detriche, J. Lambert and P. Malblanc, "The sprint of coach," *Proceedings of IEEE Systems Man and Cybernetics Conference-SMC*, vol. 3 (IEEE, 1993) pp. 547–552.
- [9] R. Simpson, E. LoPresti, S. Hayashi, S. Guo, D. Ding, W. Ammer, V. Sharma and R. Cooper, "A prototype power assist wheelchair that provides for obstacle detection and avoidance for those with visual impairments," *J. NeuroEng. Rehabil.* **2**(1), 30 (2005).
- [10] S. P. Levine, D. A. Bell, L. A. Jaros, R. C. Simpson, Y. Koren and J. Borenstein, "The navchair assistive wheelchair navigation system," *IEEE Trans. Rehabil. Eng.* **7**(4), 443–451 (1999).
- [11] C. Lauretti, F. Cordella, E. Guglielmelli and L. Zollo, "Learning by demonstration for planning activities of daily living in rehabilitation and assistive robotics," *IEEE Rob. Autom. Lett.* **2**(3), 1375–1382 (2017).
- [12] D. Schwesinger, A. Shariati, C. Montella and J. Spletzer, "A smart wheelchair ecosystem for autonomous navigation in urban environments," *Auto. Rob.* **41**(3), 519–538 (2017).
- [13] C. Mandel, T. Laue and S. Autexier, "Smart-Wheelchairs," *In: Smart Wheelchairs and Brain-Computer Interfaces* (2018) pp. 291–322.
- [14] J. Leaman and H. M. La, "A comprehensive review of smart wheelchairs: past, present, and future," *IEEE Trans. Hum. Mach. Syst.* **47**(4), 486–499 (2017).
- [15] G. Pereira, "Comparison of Human Machine Interfaces to Control a Robotized Wheelchair," *XIII Simpósio Brasileiro de Automação Inteligente - Porto Alegre, RS* (2017) pp. 2301–2306.
- [16] J. Long, Y. Li, H. Wang, T. Yu, J. Pan and F. Li, "A hybrid brain computer interface to control the direction and speed of a simulated or real wheelchair," *IEEE Trans. Neural Syst. Rehabil. Eng.* **20**(5), 720–729 (2012).
- [17] Y. Ren, Y.-N. Wu, C.-Y. Yang, T. Xu, R. L. Harvey and L.-Q. Zhang, "Developing a wearable ankle rehabilitation robotic device for in-bed acute stroke rehabilitation," *IEEE Trans. Neural Syst. Rehabil. Eng.* **25**(6), 589–596 (2016).
- [18] V. Schettino and Y. Demiris, "Inference of User-Intention in Remote Robot Wheelchair Assistance Using Multimodal Interfaces," *Proceedings of iROS2019* (to appear).
- [19] A. Escobedo, A. Spalanzani and C. Laugier, "Multimodal Control of a Robotic Wheelchair: Using Contextual Information for Usability Improvement," *International Conference on Intelligent Robots and Systems (IROS)* (IEEE, 2013) pp. 4262–4267.
- [20] J. Kim, H. Park, J. Bruce, E. Sutton, D. M. Rowles, D. Pucci, J. Holbrook, J. Minocha, B. Nardone, D. P. West, A. E. Laumann, E. J. Roth, M. Jones, E. Veledar and M. Ghovanloo, "The tongue enables computer and wheelchair control for people with spinal cord injury," *Sci. Trans. Med.* **5**(213), 166–213 (2013).
- [21] A. Naeem, A. Qadar and W. Safdar, "Voice controlled intelligent wheelchair using raspberry pi," *Int. J. Technol. Res.* **2**(2), 65 (2014).
- [22] Y. Liu, Z. Li, T. Zhang and S. Zhao, "Brain-robot interface-based navigation control of a mobile robot in corridor environments," *IEEE Trans. Syst. Man Cybern. Syst.* **50**(8), 3047–3058 (2018).
- [23] S. Ruiz-Gómez, C. Gómez, J. Poza, G. C. G. Tobal, M. A. T. Arribas, M. Cano and R. Hornero, "Automated multiclass classification of spontaneous EEG activity in Alzheimer's disease and mild cognitive impairment," *Entropy*, Multidisciplinary Digital Publishing Institute, vol. 20 (Elsevier, 2018) pp. 22–30.
- [24] E. Rohmer, P. Pinheiro, E. Cardozo, M. Bellone and G. Reina, "Laser Based Driving Assistance for Smart Robotic Wheelchairs," *2015 IEEE 20th Conference on Emerging Technologies & Factory Automation (ETFA)* (IEEE, 2015) pp. 1–4.
- [25] K. D. Shinde, S. Tarannum, T. Veerabhadrapa, E. Gagan and P. V. Kumar, "Implementation of Low Cost, Reliable, and Advanced Control with Head Movement, Wheelchair for Physically Challenged People," *In: Progress in Advanced Computing and Intelligent Engineering* (Springer, 2018) pp. 313–328.
- [26] G. Marins, D. Carvalho, A. Marcato and I. Junior, "Development of a Control System for Electric Wheelchairs Based on Head Movements," *Intelligent Systems Conference (IntelliSys)* (IEEE, 2017) pp. 996–1001.
- [27] C. Torkia, D. Reid, N. Korner-Bitensky, D. Kairy, P. W. Rushton, L. Demers and P. S. Archambault, "Power wheelchair driving challenges in the community: A users' perspective," *Disability Rehabil. Assistive Technol.* **10**(3), 211–215 (2015).
- [28] S.-H. Chen, Y.-L. Chen, Y.-H. Chiou, J.-C. Tsai and T.-S. Kuo, "Head-Controlled Device with M3S-Based for People with Disabilities," *Proceedings of the 25th Annual International Conference of the IEEE Engineering in Medicine and Biology Society (IEEE Cat. No. 03CH37439)*, vol. 2 (IEEE, 2003) pp. 1587–1589.
- [29] R. Chauhan, Y. Jain, H. Agarwal and A. Patil, "Study of Implementation of Voice Controlled Wheelchair," *2016 3rd International Conference on Advanced Computing and Communication Systems (ICACCS)*, vol. 1 (2016) pp. 1–4. doi: [10.1109/ICACCS.2016.7586329](https://doi.org/10.1109/ICACCS.2016.7586329).
- [30] X. Huo and M. Ghovanloo, "Evaluation of a wireless wearable tongue-computer interface by individuals with high-level spinal cord injuries," *J. Neural Eng.* **7**(2), 26008 (2010).
- [31] C.-S. Lin, C.-W. Ho, W.-C. Chen, C.-C. Chiu and M.-S. Yeh, "Powered wheelchair controlled by eye-tracking system.," *Optica Applicata* **36** (2006).
- [32] A. Kucukyilmaz and Y. Demiris, "Learning shared control by demonstration for personalized wheelchair assistance," *IEEE Trans. Haptics* **11**(3), 431–442 (2018).

- [33] A. Kucukyilmaz and Y. Demiris, "One-Shot Assistance Estimation from Expert Demonstrations for a Shared Control Wheelchair System," *2015 24th IEEE International Symposium on Robot and Human Interactive Communication (RO-MAN)* (IEEE, 2015) pp. 438–443.
- [34] M. F. Ruzajj, S. Neubert, N. Stoll and K. Thurow, "Multi-Sensor Robotic-Wheelchair Controller for Handicap and Quadriplegia Patients Using Embedded Technologies," *2016 9th International Conference on Human System Interactions (HSI)* (IEEE, 2016) pp. 103–109.
- [35] P. Dey, M. M. Hasan, S. Mostofa and A. I. Rana, "Smart Wheelchair Integrating Head Gesture Navigation," *2019 International Conference on Robotics, Electrical and Signal Processing Techniques (ICREST)* (IEEE, 2019) pp. 329–334.
- [36] P. Jia and H. Hu, "Head Gesture Based Control of an Intelligent Wheelchair," *Proceedings of the 11th Annual Conference of the Chinese Automation and Computing Society in the UK [CAC/SUK05]* (2005) pp. 85–90.
- [37] C. S. Teodorescu, B. Zhang and T. Carlson, "Probabilistic Shared Control for a Smart Wheelchair: A Stochastic Model-Based Framework," *2019 IEEE International Conference on Systems, Man and Cybernetics (SMC)* (2019) pp. 3136–3141.
- [38] H. H. Triharminto, O. Wahyunggoro, T. B. Adji and A. I. Cahyadi, "An integrated artificial potential field path planning with kinematic control for nonholonomic mobile robot," *Int. J. Adv. Sci. Eng. Inf. Technol.* **6**(4), 410–418 (2016).
- [39] H. Seki, S. Shibayama, Y. Kamiya and M. Hikizu, "Practical Obstacle Avoidance Using Potential Field for a Nonholonomic Mobile Robot with Rectangular Body," *International Conference on Emerging Technologies and Factory Automation* (2008) pp. 326–332.
- [40] C. Diao, S. Jia, G. Zhang, Y. Sun, X. Zhang, Y. Xue and X. Li, "Design and Realization of a Novel Obstacle Avoidance Algorithm for Intelligent Wheelchair bed Using Ultrasonic Sensors," *Chinese Automation Congress (CAC), 2017* (2017) pp. 4153–4158.
- [41] L. Olivi, R. Souza, E. Rohmer and E. Cardozo, "Shared Control for Assistive Mobile Robots Based on Vector Fields," *International Conference on Ubiquitous Robots and Ambient Intelligence (URAI)* (2013) pp. 96–101.
- [42] J. Wang, W. Chen and W. Liao, "An improved localization and navigation method for intelligent wheelchair in narrow and crowded environments," *IFAC Proc. Volumes* **46**(13), 389–394 (2013).
- [43] M. R. M. Tomari, Y. Kobayashi and Y. Kuno, "Development of smart wheelchair system for a user with severe motor impairment," *Procedia Eng.* **41**, 538–546 (2012). doi: [10.1016/j.proeng.2012.07.209](https://doi.org/10.1016/j.proeng.2012.07.209).
- [44] M. Burhanpurkar, M. Labbé, C. Guan, F. Michaud and J. Kelly, "Cheap or Robust? the Practical Realization of Self-Driving Wheelchair Technology," *International Conference on Rehabilitation Robotics (ICORR)* (2017) pp. 1079–1086.
- [45] Q. Huang, Y. Chen, Z. Zhang, S. He, R. Zhang, J. Liu, Y. Zhang, M. Shao and Y. Li, "An EOG-based wheelchair robotic arm system for assisting patients with severe spinal cord injuries," *J. Neural Eng.* **16**(2), 21–26 (2019).
- [46] H. M. Qassim, A. K. Eese, O. T. Osman and M. S. Jarjees, "Controlling a motorized electric wheelchair based on face tilting," *Bio-Algorithms Med-Syst.* **15**(4), 1–7 (2019).
- [47] M. F. Pinto, F. O. Coelho, J. P. Souza, A. G. Melo, A. L. M. Marcato and C. Urdiales, "EKF Design for Online Trajectory Prediction of a Moving Object Detected Onboard of a UAV," *2018 13th APCA International Conference on Automatic Control and Soft Computing (CONTROLO)* (IEEE, 2018) pp. 407–412.
- [48] M. M. Almasri, A. M. Alajlan and K. M. Elleithy, "Trajectory planning and collision avoidance algorithm for mobile robotics system," *IEEE Sens. J.* **16**(12), 5021–5028 (2016).
- [49] C. W. Warren, "Global Path Planning Using Artificial Potential Fields," *Proceedings, 1989 International Conference on Robotics and Automation* (1989) pp. 316–321.
- [50] M. F. Pinto, T. R. Mendonça, L. R. Olivi, E. B. Costa and A. L. Marcato, "Modified Approach Using Variable Charges to Solve Inherent Limitations of Potential Fields Method," *2014 11th IEEE/IAS International Conference on Industry Applications (INDUSCON)* (2014) pp. 1–6.
- [51] A. C. Woods and H. M. La, "A novel potential field controller for use on aerial robots," *IEEE Trans. Syst. Man Cybern. Syst.* **49**(4), 665–676 (2017).
- [52] F. O. Coelho, M. F. Pinto, J. P. C. Souza and A. L. Marcato, "Hybrid methodology for path planning and computational vision applied to autonomous mission: A new approach," *Robotica*, **38**(6), 1000–1018 (2020).
- [53] "Smart wheelchair." https://github.com/patilnabhi/nuric_wheelchair_model_02. Accessed 19th August 2019 (2016).
- [54] S. G. Hart, "Nasa-Task Load Index (NASA-TLX); 20 Years Later," *Proceedings of the Human Factors and Ergonomics Society Annual Meeting*, vol. 50 (2006) pp. 904–908.
- [55] G. M. Maciel, M. F. Pinto, I. C. da S. Júnior and A. L. M. Marcato, "Methodology for autonomous crossing narrow passages applied on assistive mobile robots," *J. Control Autom. Electr. Syst.* **30**(6), 943–953 (2019).

Cite this article: G. M. Maciel, M. F. Pinto, I. C. da S. Júnior, F. O. Coelho, A. L. M. Marcato and M. M. Cruzeiro (2022). "Shared control methodology based on head positioning and vector fields for people with quadriplegia", *Robotica* **40**, 348–364. <https://doi.org/10.1017/S0263574721000606>